



Research paper

Visible light β -Bi₂O₃/BiOCl heterojunction photocatalyst with highly enhanced photocatalytic activity

Xinde Tang*, Changsong Ma, Ning Liu, Chenglu Liu, Shuilin Liu

Department of Materials and Chemical Engineering, Hunan Institute of Technology, Hengyang 421002, China

HIGHLIGHTS

- This is a systematic study on photocatalytic property of β -Bi₂O₃/BiOCl composites.
- The composites exhibited highly enhanced activity for RhB degradation.
- The BBC-1.5 heterojunction exhibits the best visible-light photocatalytic activity.
- The heterojunctions lead to the efficient separation of electron-hole pairs.
- h^+ and $\cdot O_2^-$ were chiefly responsible for the process of RhB degradation.

ARTICLE INFO

Keywords:
 β -Bi₂O₃/BiOCl
 Heterojunction
 Photocatalyst
 Rhodamine B
 Visible light

ABSTRACT

A series of β -Bi₂O₃/BiOCl heterojunction photocatalysts were successfully synthesized by in-situ treatment of β -Bi₂O₃ with HCl. Compared to pure β -Bi₂O₃, the as-synthesized β -Bi₂O₃/BiOCl composites displayed unexpectedly high visible-light photocatalytic activity for RhB degradation, which was even higher than that of P25 under UV light. Based on the results of transient photocurrent measurement and trapping experiments of active species, the enhanced photocatalytic activity could be ascribed to the formation of heterostructure between β -Bi₂O₃ and BiOCl, leading to the efficient separation of electron-hole pairs. This research may establish foundation for practical application of the new visible-light-active β -Bi₂O₃-based heterojunction photocatalysts.

1. Introduction

In the recent decades, photocatalysis has been drawn more and more attention for offering a hopeful solution in environmental remediation [1–3]. In order to make full use of affluent solar energy, the exploitation of efficient and stable visible-light-response photocatalysts still remains challenging and urgent demand [4]. Recently, Bismuth-based compounds have drawn much attention in photocatalysis due to its unique electronic structure [5–9]. Especially, Bi₂O₃ is a potential candidate as a visible-light-response photocatalyst due to narrow band gap [10]. Bi₂O₃ exists in six polymorphic forms which are α , β , γ , δ , ϵ , and ω phases [11]. Among these, β -Bi₂O₃ has the best photocatalytic performance under visible-light irradiation [12,13]. However, β -Bi₂O₃ still needs to enhance photocatalytic efficiency for practical application in environmental protection. Therefore, further efforts need be made to obtain desired photocatalytic activity of β -Bi₂O₃. Subject to the major processes of semiconductor photocatalysis, efficient transport and separation of photoinduced electron-hole ($e^- - h^+$) pairs are crucial for

β -Bi₂O₃ to achieve high photocatalytic efficiency. To improve transport and separation of photogenerated charges and then to promote the photocatalytic activity of photocatalysts, constructing a semiconductor heterostructure by coupling with other semiconductors has been proven to be a simple and good strategy [14–16]. Actually, various β -Bi₂O₃-based heterojunctions such as β -Bi₂O₃/Bi₂O₂CO₃ [17], β -Bi₂O₃/BiOI [18], β -Bi₂O₃/TiO₂-NTs [19], β -Bi₂O₃/Bi₂MoO₆ [20], β -Bi₂O₃/Bi₂WO₆ [21], β -Bi₂O₃/ZrO₂ [22], and β -Bi₂O₃/ZnO [23] have been developed and displayed enhanced photocatalytic activity due to the efficient separation of photoinduced e^-/h^+ pairs. BiOCl has recently drawn an increasing attention in photocatalysis due to its high photocorrosion stability and unique layered-structure, which contributes to the transport and separation of the photo-induced $e^- - h^+$ pairs [24–31]. Therefore, BiOCl can be used as optimal candidate semiconductor to construct heterojunction photocatalysts. It is expected that the coupling β -Bi₂O₃ with BiOCl will be conducive to enhance the photocatalytic activity compared with β -Bi₂O₃. It has been reported that a handful of BiOCl at the surface of β -Bi₂O₃ promoted the photocatalytic activities of

* Corresponding author at: Department of Materials and Chemical Engineering, Hunan Institute of Technology, Hengyang 421002, China.
 E-mail address: txd738011@126.com (X. Tang).

<https://doi.org/10.1016/j.cplett.2018.08.045>

Received 1 July 2018; Accepted 16 August 2018

Available online 17 August 2018

0009-2614/ © 2018 Elsevier B.V. All rights reserved.

the catalysts [5]. However, it is lack of the systematic study on β - Bi_2O_3 /BiOCl. Moreover, it is absent of the compared photocatalytic performance of the β - Bi_2O_3 /BiOCl to other photocatalyst.

In this work, the visible active β - Bi_2O_3 /BiOCl heterojunction photocatalysts constructed by β - Bi_2O_3 nanorods and two-dimension BiOCl nanosheets were successfully synthesized by in-situ treatment of β - Bi_2O_3 with HCl. The photodegradation activity of the as-prepared β - Bi_2O_3 /BiOCl heterojunction photocatalyst was evaluated by degrading RhB and its reusability was investigated under visible light irradiation. Interestingly, the β - Bi_2O_3 /BiOCl heterojunction photocatalyst exhibited more excellent visible-light photodegradation activity than that of pure β - Bi_2O_3 and BiOCl, and its photocatalytic activity under visible light is even higher than that of P25 under UV light irradiation. Additionally, the β - Bi_2O_3 /BiOCl heterojunction photocatalyst was highly stable during photodegradation reaction. A possible visible-light photodegradation mechanism of RhB over β - Bi_2O_3 /BiOCl heterojunction photocatalyst was further proposed.

2. Experimental section

2.1. Synthesis of β - Bi_2O_3 /BiOCl

2.1.1. Preparation of β - Bi_2O_3

β - Bi_2O_3 was prepared by a method of precipitation and thermal treatment based on Han's work with minor modifications [18]. Firstly, 12 mmol of $\text{Bi}(\text{NO}_3)_3 \cdot 5\text{H}_2\text{O}$ was dissolved in 30 ml HNO_3 (1 mol/L) solution. Subsequently, 120 ml of Na_2CO_3 (0.6 mol/L) solution was dropwise added into the above solution under full agitation. The obtained suspension was further stirred for 30 min, and then aged at 60 °C for 12 h. Finally, the precipitates were collected and separated by centrifugation, washed with deionized water, and followed by drying at 60 °C for 12 h to obtain the white $\text{Bi}_2\text{O}_2\text{CO}_3$ precursor, which was calcined at 350 °C for 1 h to obtain the deep yellow β - Bi_2O_3 .

2.1.2. Preparation of β - Bi_2O_3 /BiOCl

The β - Bi_2O_3 /BiOCl heterojunctions were synthesized by an in-situ treatment of as-prepared β - Bi_2O_3 with HCl. Detailedly, 0.466 g of as-prepared β - Bi_2O_3 was dispersed in 40 ml of an absolute ethanol and deionized water mixtures by ultrasonic treating. Then a certain amount of 1 mol/L HCl solution was dropwise added with vigorously stirring for 3 h at room temperature. And after that, the precipitates were washed with deionized water, followed by drying in vacuum at 60 °C for 12 h. By changing the amount of HCl added in the above synthesis process, a series of β - Bi_2O_3 /BiOCl samples were prepared, and the obtained β - Bi_2O_3 /BiOCl samples are denoted as BBC-X, where X means the amount of 1 mol/L HCl solution. The content of BiOCl in BBC-0.5, BBC-1, BBC-1.5 and BBC-1.8 can be calculated as ~40 mol%, 66.7 mol%, 85.7 mol% and 94.7 mol%, respectively. In addition, pure BiOCl was also prepared with addition of excessive HCl (4 ml) by the same manner.

2.2. Material characterization

The phase compositions of the samples were determined by X-ray power diffractometer (XRD, SHIMADZU XRD-6100) with Cu K α radiation. The morphologies and microstructures of the samples were characterized by a field emission scanning electron microscope (FESEM, Nova Nano SEM 230) and a transmission electron microscopy (TEM, TECNAI G2 F20). The surface chemical states and composition of the samples were determined by X-ray photoelectron spectrometer (XPS, ESCALAB 250Xi). The optical properties of the samples were analyzed using a UV–vis spectrophotometer (UV–vis DRS, SHIMADZU UV-2700) with a diffuse reflectance accessory. The photo-electrochemical tests were performed via an electrochemical workstation (CHI 660D, China) in 0.05 M Na_2SO_4 electrolyte solution in a three-electrode cell.

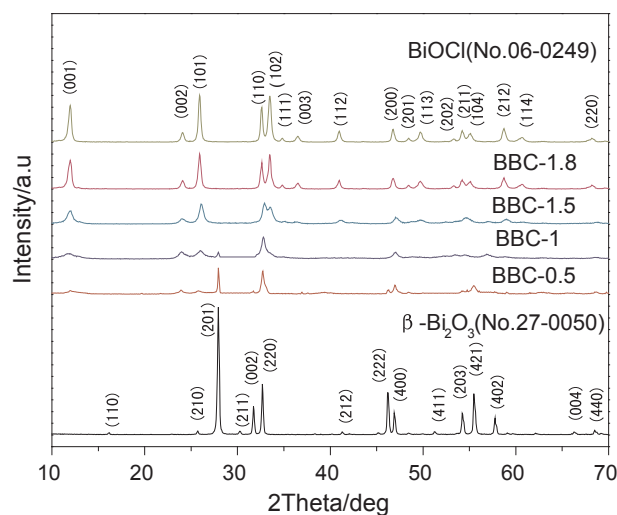


Fig. 1. XRD patterns of the as- prepared samples.

2.3. Photocatalytic measurement

The photodegradations of RhB solution were performed in a 100 ml pyrex glass vessel with a jacket at ~25 °C controlled by recirculating cooling water system. A 300 W Xe-arc lamp with a cutoff filter (400 nm < λ < 780 nm) was used as the visible-light source. In a typical process, 25 mg of photocatalyst was suspended in 50 ml of 10 mg L⁻¹ RhB aqueous solution, which was stirred for 30 min to establish equilibrium adsorption in a dark room before irradiation. 3 ml of RhB solutions were sampled at certain time intervals during irradiation and centrifuged to remove the powders. The resulting filtrates were analyzed by UV–vis spectrophotometer (UV-2700), and its concentration was determined from the peak absorbance of RhB solutions at its absorption maximum.

3. Results and discussion

3.1. Crystal structures and phase compositions

The as-prepared pure β - Bi_2O_3 , BiOCl and β - Bi_2O_3 /BiOCl were characterized by XRD. As shown in Fig. 1, β - Bi_2O_3 sample exhibits the characteristic (110), (210), (201), (211), (002), (220), (212), (222), (400), (411), (203), (411), (402), (004) and (440) planes that can be indexed to the tetragonal phase of β - Bi_2O_3 (JCPDS card no. 27-0050) [18]. After the treatment of certain amount of HCl, the diffraction peaks corresponding to BiOCl were also observed. From sample BBC-0.5 to BBC-1.8, the intensity of the main diffraction peak corresponding to β - Bi_2O_3 gradually decrease, while that of the peak corresponding to BiOCl become stronger and stronger. With treatment of excessive HCl, the crystalline β - Bi_2O_3 is thoroughly converted to the pure BiOCl, which exhibits the characteristic (001), (002), (101), (110), (102), (111), (003), (112), (200), (113), (202), (211), (104), (212), (114) and (220) reflections that can be assigned to the tetragonal form of BiOCl (JCPDS card no. 06-0249) [32].

The surface composition and chemical states of β - Bi_2O_3 , BiOCl and BBC-1.5 composites were analyzed by XPS. As seen from Fig. 2a, the survey spectrum of BBC-1.5 shows the presence of chlorine except bismuth and oxygen compared with β - Bi_2O_3 . Fig. 2b contrasts the Bi 4f spectra of β - Bi_2O_3 , BiOCl and BBC-1.5. In the Bi 4f spectrum of the β - Bi_2O_3 , two strong peaks at 158.5 and 163.8 eV are assigned to Bi 4f_{5/2} and Bi 4f_{7/2}, respectively, which correspond to Bi³⁺ [18,33]. The binding energies of Bi 4f_{5/2} and Bi 4f_{7/2} peaks in the pure BiOCl are located at 159.5 and 164.8 eV, respectively, suggesting that Bi³⁺ existed in the pure BiOCl [34]. In the Bi 4f spectrum of the BBC-1.5, the

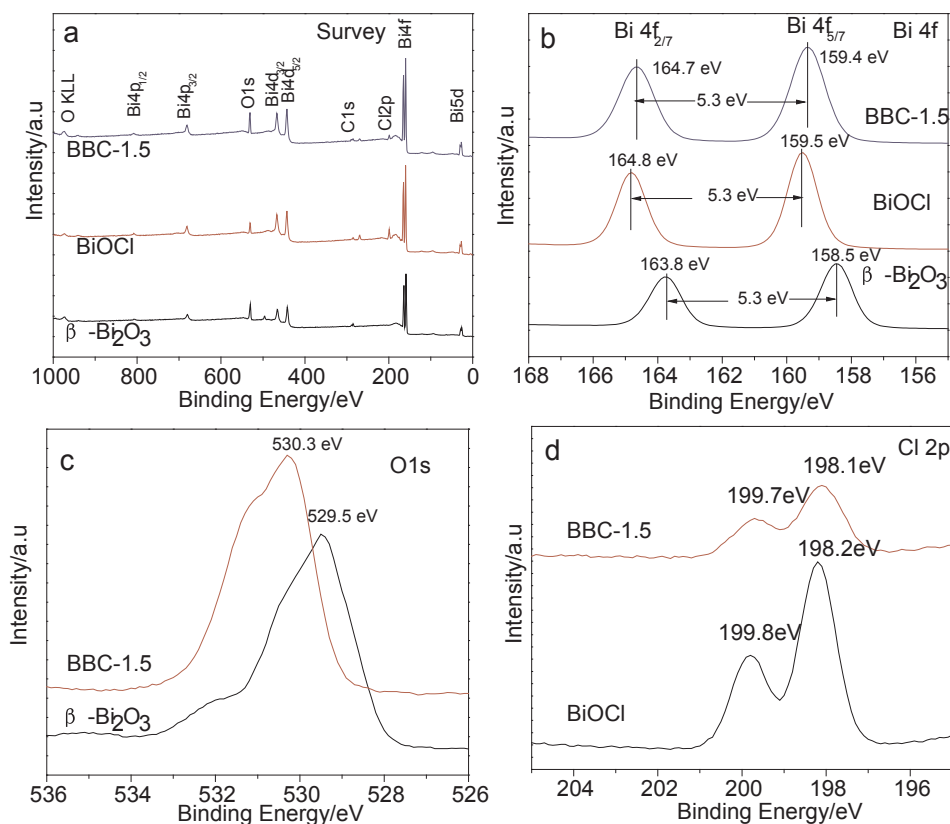


Fig. 2. XPS survey spectra (a) and Bi 4f spectra (b) of β - Bi_2O_3 , BiOCl and BBC-1.5; O 1s spectra (c) of β - Bi_2O_3 and BBC-1.5; Cl 2p spectra (d) of BiOCl and BBC-1.5.

corresponding Bi $4f_{5/2}$ and Bi $4f_{7/2}$ peaks shift to 159.4 and 164.7 eV, respectively, and the value of peak separation is still the same as that of pure β - Bi_2O_3 and BiOCl. In the XPS spectra of O 1s of the β - Bi_2O_3 (Fig. 2c), the main peak at 529.5 eV is assigned to lattice oxygen (Bi-O), and the other peaks can be ascribed to surface hydroxyl groups and adsorbed H_2O [35,36]. After β - Bi_2O_3 was in-situ treated with HCl, the binding energy of the corresponding Bi 4f and O 1s (Fig. 2b and c) obviously shift to higher values, indicating the strong interaction between β - Bi_2O_3 and BiOCl in the BBC-1.5 [37]. Fig. 2d shows the Cl 2p core-level spectrum of the pure BiOCl and BBC-1.5. The two peaks at 198.1 eV (or 198.2 eV) and 199.7 eV (or 199.8 eV) can be ascribed to the Cl $2p_{3/2}$ and $2p_{1/2}$ [38], respectively. After the formation of β - Bi_2O_3 /BiOCl heterojunctions, the binding energies of Cl $2p_{3/2}$ and $2p_{1/2}$ slightly shift to lower values, which also indicated the strong interaction between β - Bi_2O_3 and BiOCl in the BBC-1.5 [18].

3.2. Morphology and optical properties

The morphologies of pure β - Bi_2O_3 , BiOCl and β - Bi_2O_3 /BiOCl were characterized by SEM. Fig. S1 shows the typical SEM images of these products. As seen from β - Bi_2O_3 , it is made up of aggregated short nanorods with the length of about 200 nm (Fig. S1a). After the treatment of HCl, some nanosheets, which can be ascribed to BiOCl according to XRD and XPS results, can be observed to grow in situ on the surface of β - Bi_2O_3 (Fig. S1b). The in-situ growth should build close connection between β - Bi_2O_3 and BiOCl, which contributes to the transport of photogenerated charges [38]. As shown in Fig. S1b–e, when the dosage of HCl increases, the amount of β - Bi_2O_3 nanorods and BiOCl nanosheets gradually decreases and increases, respectively. With the addition of excessive HCl, the irregular pure BiOCl nanosheets with a smooth surface are formed (Fig. S1f). The detailed structural information of β - Bi_2O_3 /BiOCl was characterized by TEM. Fig. 3 exhibits the low-

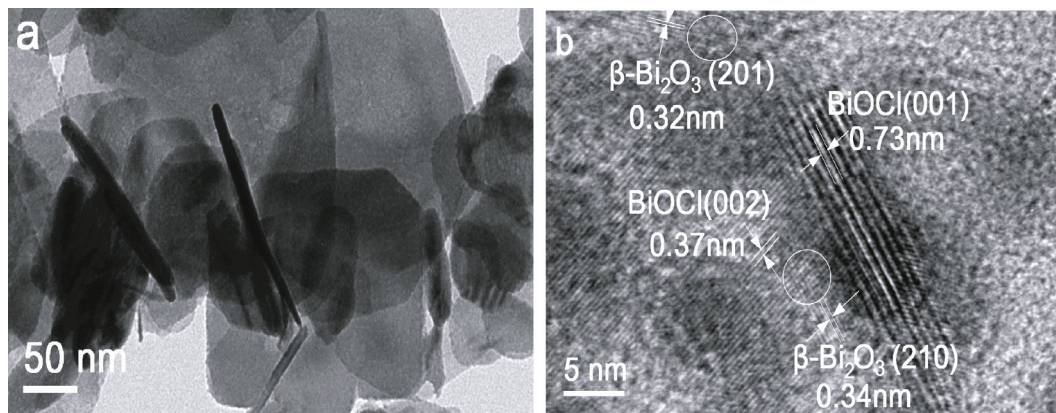


Fig. 3. Low-magnification TEM images (a) and HRTEM images (b) of BBC-1.5.

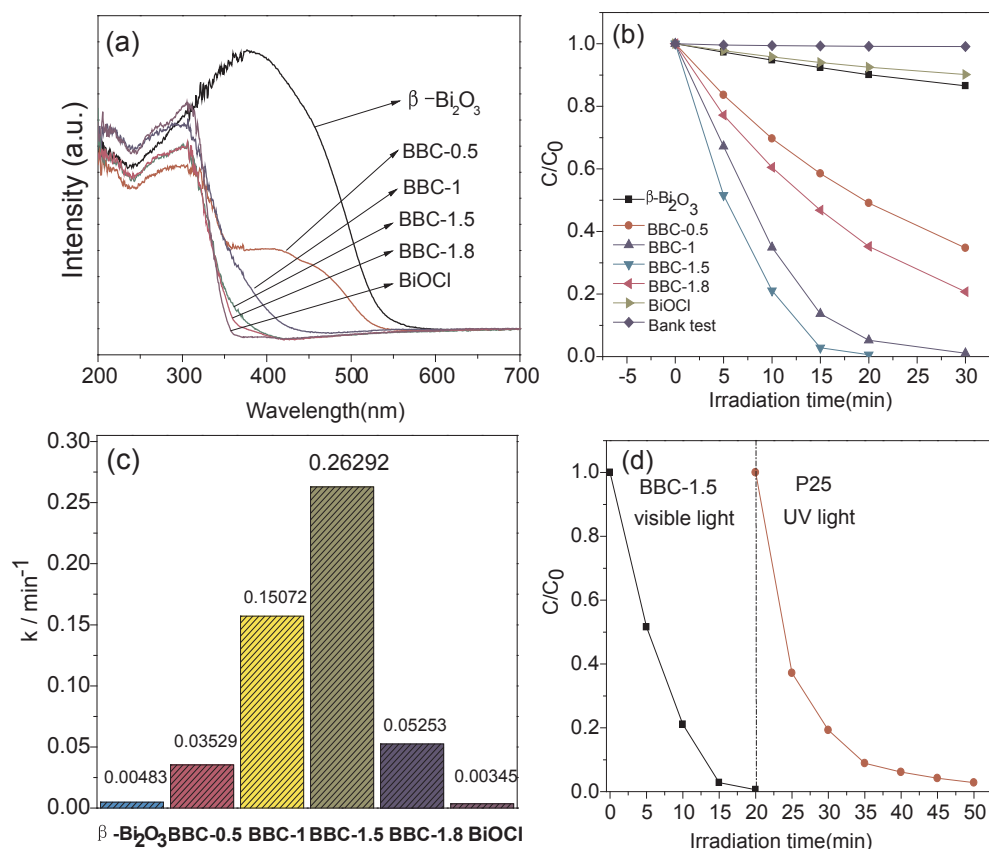


Fig. 4. (a) The UV-vis DRS of pure BiOCl, β - Bi_2O_3 and β - Bi_2O_3 /BiOCl heterojunction photocatalysts; (b) Photodegradation curves of RhB over BiOCl, β - Bi_2O_3 and β - Bi_2O_3 /BiOCl heterojunction catalysts under visible light irradiation; (c) The apparent first-order rate constants (k) of BiOCl, β - Bi_2O_3 and β - Bi_2O_3 /BiOCl heterojunction catalysts for RhB degradation; (d) Photodegradation curves of RhB over BBC-1.5 and P25.

magnification TEM and high resolution TEM (HRTEM) images of the representational BBC-1.5 sample. As shown in Fig. 3a, the BBC-1.5 composites are composed of a small number of β - Bi_2O_3 nanorods and many BiOCl nanosheets. Besides, the HRTEM image (Fig. 3b) of BBC-1.5 composites clearly displays the lattice spacing of 0.32 nm, 0.34 nm, 0.37 nm and 0.73 nm corresponded to the (201) and (210) planes of tetragonal β - Bi_2O_3 and (002) and (001) planes of tetragonal BiOCl [16,18,39,40], respectively. Especially, some cross lattice fringes marked by white circles are found, which indicated the successful formation of heterojunctions between β - Bi_2O_3 and BiOCl [41].

Supplementary data associated with this article can be found, in the online version, at <https://doi.org/10.1016/j.cplett.2018.08.045>.

Fig. 4a displays the UV-vis DRS of pure β - Bi_2O_3 , BiOCl and β - Bi_2O_3 /BiOCl heterojunction photocatalysts. The β - Bi_2O_3 shows strong visible-light absorption and its absorption edge is about 540 nm, while pure BiOCl only displays UV-light absorption with an absorption edge of about 360 nm. Thus, the band gap energy of pure β - Bi_2O_3 and BiOCl can be calculated to be 2.29 and 3.44 eV, respectively. After the β - Bi_2O_3 is couple with BiOCl to form heterojunctions, the absorption edge of the heterojunctions is gradually blue-shifted¹ with the increasing of BiOCl due to the large band gap of BiOCl.

3.3. Photocatalytic properties

The photocatalytic activity of BiOCl, β - Bi_2O_3 and β - Bi_2O_3 /BiOCl composites was investigated by the degradation of cationic dye RhB under visible light irradiation. As shown in Fig. 4b, the RhB can be hardly degraded without any photocatalyst (blank). After 30 min of

irradiation, the pure BiOCl and β - Bi_2O_3 only removed about 9.8% and 13.4% of RhB, respectively. However, the photodegradation activity was obviously enhanced with β - Bi_2O_3 /BiOCl heterojunction formed. The BiOCl content has crucial effect on the photocatalytic activity of β - Bi_2O_3 /BiOCl photocatalyst, and the BBC-1.5 has displayed the highest photodegradation activity among six catalysts. Nearly complete degradation (99.4%) of RhB over BBC-1.5 can be achieved within 20 min of illumination. To further illustrate the enhancement, the pseudo-first-order model, which is generally used to research the kinetics in photodegradation reactions, was utilized to quantify the degradation rates. As shown in Fig. 4c, the value of apparent rate constant (k) for pure β - Bi_2O_3 , BBC-0.5, BBC-1, BBC-1.5, BBC-1.8 and pure BiOCl is 0.00483, 0.03529, 0.15702, 0.26292, 0.05253 and 0.00345 min^{-1} , respectively. This result showed that all β - Bi_2O_3 /BiOCl composites exhibited far higher photodegradation activity than that of pure β - Bi_2O_3 and BiOCl, and the photodegradation activity of BBC-1.5 was about 54.4 and 76.2 times higher than that of pure β - Bi_2O_3 and BiOCl, respectively. It is worth noting that the maximum absorbance of RhB showed blue shift to shorter wavelength during the degradation process due to the N-deethylation of RhB (Fig. S2) [42,43]. These above photodegradation results confirmed that β - Bi_2O_3 coupled with BiOCl could greatly enhance the photocatalytic activity.

To further display the high photodegradation activity of BBC-1.5, the photocatalytic activity of the commercial TiO_2 (P25) was studied under UV light (254 nm) and used as a comparison. As shown in Fig. 4d. After 30 min of UV (254 nm) irradiation, the photodegradation rate of RhB over P25 was about 97.2%. The results showed the photodegradation activity of BBC-1.5 under visible light was even higher than that of P25 under UV light.

To evaluate the stability of the β - Bi_2O_3 /BiOCl heterojunction photocatalyst, the repeated experiments for degrading RhB solution were performed. As shown in Fig. S3a, the photodegradation activity of the

¹ For interpretation of color in Fig. 4, the reader is referred to the web version of this article.

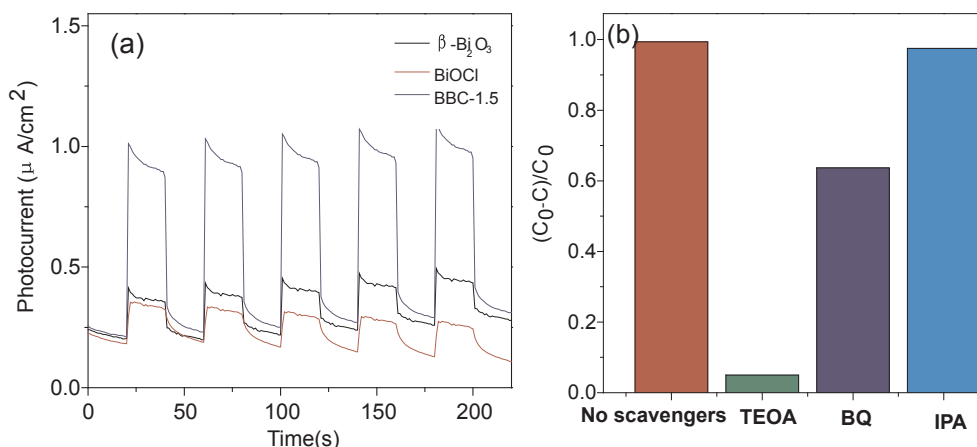


Fig. 5. (a) Transient photocurrent responses of β - Bi_2O_3 , BiOCl and BBC-1.5; (b) Effect of scavengers on the photodegradation of RhB over BBC-1.5 catalyst.

BBC-1.5 catalyst is only slight deactivation after five cycles. Moreover, Fig. S3b shows that the structure of BBC-1.5 composite also has no detectable change before and after consecutive reuse for five cycles, which indicate its high chemical stability.

3.4. Photodegradation mechanism

It is generally recognized that the activity of a photocatalyst is chiefly related to the separation and migration ability of photoinduced e^-/h^+ pairs [44]. The transient photocurrent measurement is an effective technique to study the transfer properties of photoinduced charge. Universally, the higher the photocurrent density is, the more efficient separation efficiency of photo-induced charge carriers is, and then the more efficient the photocatalytic activity is. Fig. 5a shows the photocurrent density of the as-prepared samples. The BBC-1.5 heterojunction exhibited a higher photocurrent response compared to pure β - Bi_2O_3 and BiOCl, indicating the more efficient separation efficiency over it due to the heterojunction formation between β - Bi_2O_3 and BiOCl, which had been actually confirmed by their photocatalytic activity.

In order to confirm the generation of active species during the photodegradation process of RhB over BBC-1.5, the trapping tests of active species were performed. Triethanolamine (TEOA), isopropyl alcohol (IPA) and benzoquinone (BQ) were used as the scavenger of h^+ , $\cdot\text{OH}$ and $\cdot\text{O}_2^-$, respectively. As shown in Fig. 5b, the addition of scavenger IPA can hardly decrease the photodegradation activity of RhB, indicating the absence of $\cdot\text{OH}$ radicals during photodegradation process. However, the addition of scavenger TEOA almost completely inhibited the photodegradation activity of RhB, and the addition of scavenger BQ also clearly decreased the photodegradation activity of RhB, which showed that h^+ and $\cdot\text{O}_2^-$ were the main active species during the photodegradation process of RhB over BBC-1.5 under visible light irradiation. Moreover, h^+ played a more important role than $\cdot\text{O}_2^-$ radicals.

Based upon the above discussed results and indirect dye photosensitization, a possible mechanism for the visible-light photodegradation of RhB over β - Bi_2O_3 /BiOCl heterojunction photocatalyst was proposed and illustrated in Fig. 6. The conduction band (CB) and valence band (VB) potentials of β - Bi_2O_3 are about 0.30 and 2.59 eV, respectively, and that of BiOCl are at about -1.10 and 2.40 eV, respectively [18,40]. With a narrow band gap (2.29 eV), β - Bi_2O_3 can be excited by the visible photons to produce e^- and h^+ . Because the CB potential of the β - Bi_2O_3 is more positive than that of $\text{O}_2/\cdot\text{O}_2^-$ (-0.33 eV) [45,46], the e^- on the CB of β - Bi_2O_3 cannot react with dissolved O_2 to generate $\cdot\text{O}_2^-$. Depend on the more positive potential of VB of β - Bi_2O_3 to that of BiOCl, the h^+ on the VB of β - Bi_2O_3 can transfer to the VB of BiOCl through the heterojunction formed at their interfaces, resulting in the efficient separation of $e^- - h^+$ pairs. Moreover,

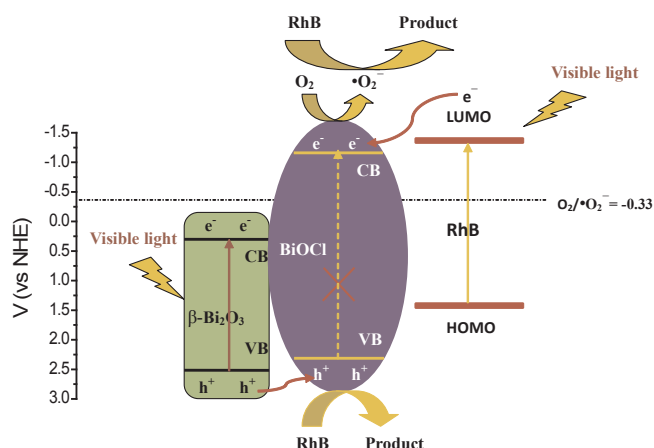


Fig. 6. Proposed mechanism for the visible light photodegradation of RhB over β - Bi_2O_3 /BiOCl heterojunction photocatalyst.

RhB molecules adsorbed on the surface of photocatalysts are sensitized by visible light to produce e^- , and the e^- transfer to the CB of BiOCl crystallites due to the more negative potential of RhB lowest unoccupied molecular orbital (LUMO) level [27]. The e^- that migrated to the CB of BiOCl can react with dissolved O_2 to generate $\cdot\text{O}_2^-$ due to more negative CB potential than that of $\text{O}_2/\cdot\text{O}_2^-$. Finally, these photoinduced h^+ and generated $\cdot\text{O}_2^-$ radicals can oxidize adsorbed RhB molecules, which induce RhB dye decomposition. Thus, it is considered for the β - Bi_2O_3 /BiOCl that BiOCl works as a prime photocatalyst, and β - Bi_2O_3 plays the role of a sensitizer absorbing visible light.

4. Conclusion

β - Bi_2O_3 /BiOCl heterojunction photocatalysts were successfully prepared by a precipitation method, followed by an in-situ treatment with HCl. Compared with pure β - Bi_2O_3 and BiOCl, the as-prepared β - Bi_2O_3 /BiOCl heterojunction photocatalysts had displayed highly enhanced visible-light photocatalytic activity in decomposing RhB due to the formation of heterostructure between β - Bi_2O_3 and BiOCl, resulting in the efficient separation of $e^- - h^+$ pairs. The photodegradation activity of β - Bi_2O_3 /BiOCl under visible light was even higher than that of P25 under UV light. The reusable experiments showed that the β - Bi_2O_3 /BiOCl heterojunction photocatalyst was stable. The results of trapping tests showed that photogenerated holes (h^+) and superoxide radicals ($\cdot\text{O}_2^-$) were the main active species during the degradation process. In the β - Bi_2O_3 /BiOCl composites, BiOCl acts as a prime photocatalyst and β - Bi_2O_3 plays the role of a photosensitizer absorbing visible light.

Acknowledgement

This work was funded by the Hunan Provincial Natural Science Foundation of China (No. 2015JJ2043) and Hunan Provincial Department of education project (No. 2015C0356).

References

- [1] L.J. Cheng, Y. Kang, Bi₅O₇I/Bi₂O₃ composite photocatalyst with enhanced visible light photocatalytic activity, *Catal. Commun.* 72 (2015) 16–19.
- [2] E. Kowalska, K. Yoshiiri, Z.S. Wei, S.Z. Zheng, E. Kastl, H. Remita, B. Ohtani, S. Rau, Hybrid photocatalysts composed of titania modified with plasmonic nanoparticles and ruthenium complexes for decomposition of organic compounds, *Appl. Catal. B: Environ.* 178 (2015) 133–143.
- [3] X.X. Li, S.M. Fang, L. Ge, C.C. Han, P. Qiu, W.L. Liu, Synthesis of flower-like Ag/AgCl-Bi₂MoO₆ plasmonic photocatalysts with enhanced visible-light photocatalytic performance, *Appl. Catal. B: Environ.* 176–177 (2015) 62–69.
- [4] C.C. Chen, W.H. Ma, J.C. Zhao, Semiconductor-mediated photodegradation of pollutants under visible-light irradiation, *Chem. Soc. Rev.* 39 (2010) 4206–4219.
- [5] Y. Lu, Y. Zhao, Y.H. Jz Zhao, Z.F. Song, F.F. Huang, N. Gao, Y.W. Li Li, Induced aqueous synthesis of metastable β-Bi₂O₃ microcrystals for visible-light photocatalyst study, *Cryst. Growth Des.* 15 (2015) 1031–1042.
- [6] J.R. Jin, T. He, Facile synthesis of Bi₂S₃ nanoribbons for photocatalytic reduction of CO₂ into CH₃OH, *Appl. Surf. Sci.* 394 (2017) 364–370.
- [7] G.S. Zhao, W. Liu, J.Y. Li, Q.Y. Lv, W.X. Li, L.T. Liang, Facile synthesis of hierarchically structured BiVO₄ oriented along (010) facets with different morphologies and their photocatalytic properties, *Appl. Surf. Sci.* 390 (2016) 531–539.
- [8] Y.C. Hao, X.L. Dong, S.R. Zhai, X.Y. Wang, H.C. Ma, X.F. Zhang, Controllable self-assembly of a novel Bi₂MoO₆-based hybrid photocatalyst: excellent photocatalytic activity under UV, visible and near-infrared irradiation, *Chem. Commun.* 52 (2016) 6525–6528.
- [9] M. Li, J.Y. Zhang, H. Gao, F. Li, S.E. Lindquist, N.Q. Wu, R.M. Wang, Microsized BiOCl square nanosheets as ultraviolet photodetectors and photocatalysts, *ACS Appl. Mater. Interf.* 8 (2016) 6662–6668.
- [10] D.Y. Qu, L.L. Wang, D. Zheng, L. Xiao, B.H. Deng, D.Y. Qu, An asymmetric supercapacitor with highly dispersed nano-Bi₂O₃ and active carbon electrodes, *J. Power Sour.* 269 (2014) 129–135.
- [11] K. Brezesinski, R. Ostermann, P. Hartmann, J. Perlich, T. Brezesinski, Exceptional photocatalytic activity of ordered mesoporous β-Bi₂O₃ thin films and electrospun nanofiber mats, *Chem. Mater.* 22 (2010) 3079–3085.
- [12] H.F. Cheng, B.B. Huang, J.B. Lu, Z.Y. Wang, B. Xu, X.Y. Qin, X.Y. Zhang, Y. Dai, Synergistic effect of crystal and electronic structures on the visible-light-driven photocatalytic performances of Bi₂O₃ polymorphs, *Phys. Chem. Chem. Phys.* 12 (2010) 15468–15475.
- [13] M. Schlesinger, S. Schulze, M. Hietschold, M. Mehring, Metastable β-Bi₂O₃ nanoparticles with high photocatalytic activity from polynuclear bismuth oxido clusters, *Dalton Trans.* 42 (2013) 1047–1056.
- [14] J. Zhang, Q. Xu, Z.C. Feng, M.J. Li, C. Li, Importance of the relationship between surface phases and photocatalytic activity of TiO₂, *Angew. Chem. Int. Ed.* 47 (2008) 1766–1769.
- [15] T.H. Yang, Y.W. Harn, L.D. Huang, M.Y. Pan, W.C. Yen, M.C. Chen, C.C. Lin, P.K. Wei, Y.L. Chueh, J.M. Wu, Fully integrated Ag nanoparticles/ZnO nanorods/graphene heterostructured photocatalysts for efficient conversion of solar to chemical energy, *J. Catal.* 329 (2015) 167–176.
- [16] A. Hameed, T. Montini, V. Gombac, P. Fornasiero, Surface phases and photocatalytic activity correlation of Bi₂O₃/Bi₂O_{4-x} nanocomposite, *J. Am. Chem. Soc.* 130 (2008) 9658–9659.
- [17] R.P. Hu, X. Xiao, S.H. Tu, X.X. Zuo, J.M. Nan, Synthesis of flower-like heterostructured β-Bi₂O₃/Bi₂O₂CO₃ microspheres using Bi₂O₂CO₃ self-sacrifice precursor and its visible-light-induced photocatalytic degradation of o-phenylphenol, *Appl. Catal. B: Environ.* 163 (2015) 510–519.
- [18] S. Han, J. Li, K. Yang, J. Lin, Fabrication of a β-Bi₂O₃/BiOI heterojunction and its efficient photocatalysis for organic dye removal, *Chinese J. Catal.* 36 (2015) 2119–2126.
- [19] D. Li, Y. Zhang, X. Zhou, S. Guo, Fabrication of bidirectionally doped β-Bi₂O₃/TiO₂-NTs with enhanced photocatalysis under visible light irradiation, *J. Hazard. Mater.* 258 (2013) 42–49.
- [20] Y. Xu, Z. Zhang, W. Zhang, Facile preparation of heterostructured Bi₂O₃/Bi₂MoO₆ hollow microspheres with enhanced visible-light-driven photocatalytic and antimicrobial activity, *Mater. Res. Bull.* 48 (2013) 1420–1427.
- [21] M. Gui, W. Zhang, Q. Su, C. Chen, Preparation and visible light photocatalytic activity of Bi₂O₃/Bi₂WO₆ heterojunction photocatalysts, *J. Solid State Chem.* 184 (2011) 1977–1982.
- [22] K. Vignesh, R. Priyanka, M. Rajarajan, A. Suganthi, Photoreduction of Cr (VI) in water using Bi₂O₃-ZrO₂ nanocomposite under visible light irradiation, *Mater. Sci. Eng. B* 178 (2013) 149–157.
- [23] S. Park, J. Jun, H.W. Kim, C. Lee, Preparation of one dimensional Bi₂O₃-core/ZnO-shell structures by thermal evaporation and atomic layer deposition, *Solid State Commun.* 149 (2009) 315–318.
- [24] H. Gnayem, Y. Sasson, Hierarchical nanostructured 3D flowerlike BiOCl_{1-x}Br_{1-x} semiconductors with exceptional visible light photocatalytic activity, *ACS Catal.* 3 (2013) 186–191.
- [25] W. Zhang, Q. Zhang, F. Dong, Visible-light photocatalytic removal of NO in air over BiOX (X = Cl, Br, I) single-crystal nanoplates prepared at room temperature, *Ind. Eng. Chem. Res.* 52 (2013) 6740–6746.
- [26] K. Zhang, C. Liu, F. Huang, C. Zheng, W. Wang, Study of the electronic structure and photocatalytic activity of the BiOCl photocatalyst, *Appl. Catal. B: Environ.* 68 (2006) 125–129.
- [27] X.F. Chang, M.A. Gondal, A.A. Al-Saadi, M.A. Ali, H.F. Shen, Q. Zhou, J. Zhang, M.P. Du, Y.S. Liu, G.B. Ji, Photodegradation of Rhodamine B over unexcited semiconductor compounds of BiOCl and BiOBr, *J. Coll. Interf. Sci.* 377 (2012) 291–298.
- [28] S. Shenawi-Khalil, V. Uvarov, E. Menes, I. Popov, Y. Sasson, New efficient visible light photocatalyst based on heterojunction of BiOCl–Bismuth oxyhydrate, *Appl. Catal. A: Gen.* 413–414 (2012) 1–9.
- [29] L. Ye, L. Zan, L. Tian, T. Peng, J. Zhang, The 001 facets-dependent high photocatalytic activity of BiOCl nanosheets, *Chem. Commun.* 47 (2011) 6951–6953.
- [30] L. Ye, K. Deng, F. Xu, L. Tian, T. Peng, L. Zan, Increasing visible-light absorption for photocatalysis with black BiOCl, *Phys. Chem. Chem. Phys.* 14 (2012) 82–85.
- [31] L. Ye, Y. Su, X. Jin, H. Xie, C. Zhang, Recent advances in BiOX (X = Cl, Br and I) photocatalysts: synthesis, modification, facet effects and mechanisms, *Environ. Sci. Nano.* 1 (2014) 90–112.
- [32] L. Ji, H. Wang, R. Yu, Heterogeneous photocatalysts BiOX/NaBiO₃ (X = Cl, Br, I): Photo-generated charge carriers transfer property and enhanced photocatalytic activity, *Chem. Phys.* 478 (2016) 14–22.
- [33] Y.B. Ding, F. Yang, L.H. Zhu, N. Wang, H.Q. Tang, Bi³⁺ self doped NaBiO₃ nanosheets: facile controlled synthesis and enhanced visible light photocatalytic activity, *Appl. Catal. B: Environ.* 164 (2015) 151–158.
- [34] Z. He, Y. Shi, C. Gao, L. Wen, J. Chen, S. Song, BiOCl/BiVO₄ p–n heterojunction with enhanced photocatalytic activity under visible-light irradiation, *J. Phys. Chem. C* 118 (2014) 389–398.
- [35] Y. Cong, Y. Ji, Y. Ge, H. Jin, Y. Zhang, Q. Wang, Fabrication of 3D Bi₂O₃-BiOI heterojunction by a simple dipping method: Highly enhanced visible-light photoelectrocatalytic activity, *Chem. Eng. J.* 307 (2017) 572–582.
- [36] X. Meng, Z. Zhang, Facile synthesis of BiOBr/Bi₂WO₆ heterojunction semiconductors with high visible-light-driven photocatalytic activity, *J. Photochem. Photobiol. A* 310 (2015) 33–44.
- [37] Y. Chen, G. Tian, Y. Shi, Y. Xiao, H. Fu, Hierarchical MoS₂/Bi₂MoO₆ composites with synergistic effect for enhanced visible photocatalytic activity, *Appl. Catal. B: Environ.* 164 (2015) 40–47.
- [38] L. Yu, X. Zhang, G. Li, Y. Cao, Y. Shao, D. Li, Highly efficient Bi₂O₂CO₃/BiOCl photocatalyst based on heterojunction with enhanced dye-sensitization under visible light, *Appl. Catal. B: Environ.* 187 (2016) 301–309.
- [39] J. Jiang, K. Zhao, X. Xiao, L. Zhang, Synthesis and facet-dependent photoreactivity of BiOCl single-crystalline nanosheets, *J. Am. Chem. Soc.* 134 (2012) 4473–4476.
- [40] S.Y. Chai, Y.J. Kim, M.H. Jung, A.K. Chakraborty, D. Jung, W.I. Lee, Heterojunctioned BiOCl/Bi₂O₃, a new visible light photocatalyst, *J. Catal.* 262 (2009) 144–149.
- [41] X. Liu, Z. Xing, Y. Zhang, Z. Li, X. Wu, S. Tan, X. Yu, Q. Zhu, W. Zhou, Fabrication of 3D flower-like black N-TiO_{2-x}@MoS₂ for unprecedented -high visible-light-driven photocatalytic performance, *Appl. Catal. B: Environ.* 201 (2017) 119–127.
- [42] Z.S. Seddigi, M.A. Gondal, S.G. Rashid, M.A. Abdulaziz, S.A. Ahmed, Facile synthesis and catalytic performance of nanosheet-nanorods g-C₃N₄-Bi₂WO₆ heterojunction catalyst and effect of silver nanoparticles loading on bare Bi₂WO₆ and g-C₃N₄-Bi₂WO₆ for N-deethylation process, *J. Mol. Catal. A: Chem.* 420 (2016) 167–177.
- [43] S. Li, D.D. Meng, L.B. Hou, D.J. Wang, T.F. Xie, The surface engineering of CdS nanocrystal for photocatalytic reaction: a strategy of modulating the trapping states and radicals generation towards RhB degradation, *Appl. Surf. Sci.* 371 (2016) 164–171.
- [44] H. Kim, P. Borse, W. Choi, J. Lee, Photocatalytic nanodiodes for visible-light photocatalysis, *Angew. Chem. Int. Ed.* 44 (2005) 4585–4589.
- [45] Z.Y. Wang, Y. Huang, W.K. Ho, J.J. Cao, Z.X. Shen, S.C. Lee, Fabrication of Bi₂O₂CO₃/g-C₃N₄ heterojunctions for efficiently photocatalytic NO in air removal: in-situ self-sacrificial synthesis, characterizations and mechanistic study, *Appl. Catal. B: Environ.* 199 (2016) 123–133.
- [46] C.L. Yu, W.Q. Zhou, L.H. Zhu, G. Li, K. Yang, R.C. Jin, Integrating plasmonic Au nanorods with dendritic like α-Bi₂O₃/Bi₂O₂CO₃ heterostructures for superior visible-light-driven photocatalysis, *Appl. Catal. B: Environ.* 184 (2016) 1–11.